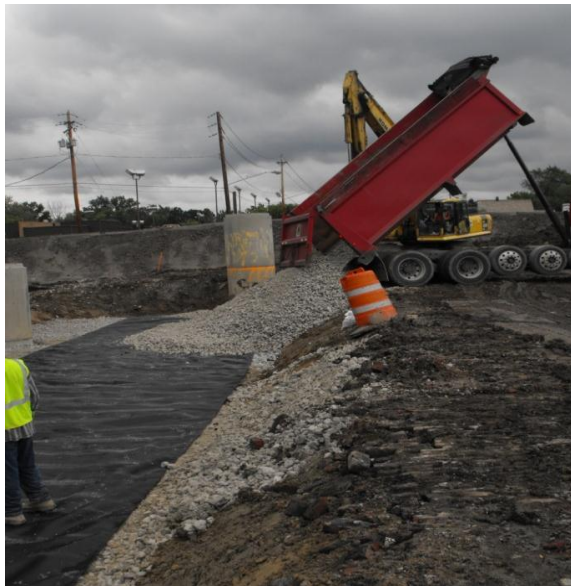


Evaluation of Geofabric in Undercut on MSE Wall Stability

*Lutful I. Khan Ph.D., P.E.
Cynthia Pearson*



Prepared for the
Ohio Department of Transportation
Office of Research and Development

State Job Number 134396

April, 2011



Cleveland State University



1. Report No. FHWA/OH-2011/2		2. Government Accession No.		3. Recipient's Catalog No.	
4. Title and subtitle Evaluation of Geofabric in Undercut on MSE Wall Stability				5. Report Date April, 2011	
				6. Performing Organization Code	
7. Author(s) Lutful Khan, Ph.D, PE Cynthia Pearson				8. Performing Organization Report No.	
9. Performing Organization Name and Address Cleveland State University Civil & Environmental Engineering Cleveland, OH 44115				10. Work Unit No. (TRAIS)	
12. Sponsoring Agency Name and Address Ohio Department of Transportation 1980 West Broad Street Columbus, Ohio 43223				11. Contract or Grant No. 134396	
				13. Type of Report and Period Covered	
				14. Sponsoring Agency Code	
15. Supplementary Notes					
16. Abstract Compaction of granular base materials at sites with fine grained native soils often causes unwanted material loss due to penetration at the base. In 2007, ODOT began placing geotextile fabrics in the undercut of MSE walls at the interface of the native soil and aggregate fill to facilitate construction. It is probable that the sliding resistances of the MSE retaining walls are affected by this practice. At this time, it is unknown if shear parameters at the base of the MSE walls are altered due to the presence of geotextiles at the soil/stone (granular backfill) interface and, if the factor of safety (FS) against sliding failure is compromised. To address this issue, a systematic investigation of the shear parameters at the geotextile/stone interface and native-soil/stone interface was conducted by Large Scale Direct Shear tests. It was observed that the shear strength between the geofabric/stone interfaces were lower than those of the soil/stone interfaces. The extent of the shear reduction depended on the properties of the base soil. For the same stone, the shear parameters at the geofabric interface changed from those of the cohesive soil interface such that friction angle slightly increased and the adhesion slightly decreased. However, the net shear strength at the geofabric interface, calculated with 25 psi normal stress, was generally lower. In case of cohesionless base soil, the shear parameters at the geofabric/stone interface reduced noticeably from those of soil/stone interface. This, in turn, produced a significant (up to 30%) reduction in shear strength at the geofabric/stone interface, calculated under 25 psi normal pressure. The findings of this research indicate that the design of MSE walls with geofabric at the undercut may require modification of the sliding safety factor to reflect the reduced shear strength at the interface.					
17. Key Words MSE wall, Geofabric friction, Large Scale Shear test, Sliding resistance				18. Distribution Statement No restrictions. This document is available to the public through the National Technical Information Service, Springfield, Virginia 22161	
19. Security Classif. (of this report) Unclassified		20. Security Classif. (of this page) Unclassified		22. Price	
Form DOT F 1700.7 (8-72)		21. No. of Pages : 29			
Reproduction of completed pages authorized					

Evaluation of Geofabric in Undercut on MSE Wall Stability

Lutful I. Khan Ph.D., P.E.
Associate Professor
Civil & Environmental Engineering Department
Cleveland State University
Cleveland, Ohio 44115
Email: l.khan@csuohio.edu
Tel: 216-687-2231

Cynthia Pearson
Graduate Assistant
Civil & Environmental Engineering Department
Cleveland State University
Cleveland, Ohio 44149
February 2011



Cleveland State University

Prepared in cooperation with the Ohio Department of Transportation and the U.S. Department Transportation, Federal Highway Administration.

The contents of this report reflect the views of the authors who are responsible for the facts and the accuracy of the data presented herein. The contents do not necessarily reflect the official views or policies of the Ohio Department of Transportation or the Federal Highway Administration. This report does not constitute a standard, specification or regulation.

Table of Contents

Introduction	4
Objectives of the Study	5
Importance of Research	5
Literature Review	5
Materials and Methods.....	5
Granular Material.....	6
Geofabrics	6
Base Soil	7
Direct Shear Test.....	7
Large Scale Direct Shear Apparatus	7
Geofabric Assembly	8
Calibration.....	9
Sample Preparation	9
Tests	10
Data & Analysis	10
Discussions.....	20
Conclusions	24
Implementation	24
Acknowledgements.....	25
REFERENCES.....	25
APPENDIX - A.....	27
APPENDIX - B.....	28

Introduction

Compaction of granular base materials at sites with fine grained native soils often causes unwanted material loss due to penetration. In 2007, ODOT began placing geofabrics in the undercut of MSE walls at the interface of the native soil and the aggregate fill (Figure 1) to facilitate construction. It is probable that the sliding resistances of the retaining walls are affected by this practice. At this time, it is unknown how the frictional resistances at the base of the MSE walls change by the addition of geofabrics at the soil/stone interface and, if the factor of safety (FS) against sliding failure is compromised. It is essential to verify the reliability of this practice because serious financial and safety consequences could result if these walls should fail.

To address this issue, a systematic investigation of the frictional resistance change due to the introduction of geofabric sheets between granular backfill material and native base soils was conducted by Large Scale Direct Shear test, a standard testing method employed for the estimation of soil shear strength parameters. An important advantage of this test is that it is possible to test larger soil samples with relative ease, and soils with large particle sizes can be tested under conditions that more closely approximate those in the field. Direct shear testing was first used by Coulomb in 1776 (Lamb and Whitman 1969), and has long been used to estimate the soil strength parameters for the analysis of slope stability, retaining wall, and bearing capacity problems. More recently, direct shear testing techniques have been extended to measure interface friction between soils and reinforcing elements in reinforced soil applications (Hausmann 1990; Lee and Manjunath 2000).

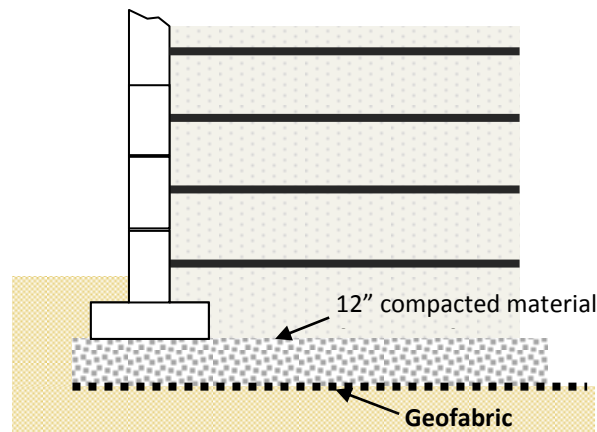


Figure 1: Placement of *Geofabric* at the MSE wall undercut.

Objectives of the Study

The objective of the proposed research was to determine how the presence of geofabrics affected the shear strength parameters, primarily the friction angle, at the MSE wall undercuts. To evaluate this, the shear strength parameters were evaluated between geofabric and stone and compared with those of base soil and stone interface. The investigation was carried out by means of a series of Large Scale Direct Shear (LSDS) tests performed in the laboratory at Cleveland State University.

Importance of Research

Several key benefits are anticipated from the findings of this research. Of these, explicit evaluation of the safety factor against sliding (FS_{sliding}) is at the forefront. As of now, there is no documentation in existence to support the current design procedure. The findings of this research will either serve as documentation to validate the current design procedure or, provide recommendations as design adjustments to insure the safety of MSE walls built in the future. Further financial savings could also result from identifying alternative geofabrics that could reduce material costs. A detailed procedure on determining the change in friction angle values will be developed for future use by other interested agencies.

Literature Review

The literature review did not expose any information on the use of a geofabric in the base of the undercut for MSE wall designs. The only known documentation of this practice is the OTEC PowerPoint presentation done by Peter Narsavage. Very few published literature exists regarding direct shear test of soil/geofabric interface with large aggregates base in large scale shear apparatus.

Wang Yi-min, et. al (2008) conducted a research to evaluate the shear stress-displacement behavior between a geocell reinforced silty gravel soil, an unreinforced silty gravel soil, a geocell reinforced cement stabilizing silty gravel soil by the direct shear method. The results from this study revealed that the large scale direct shear test produces a much higher cohesion than the triaxial tests. However, the value for the friction angle was relatively unchanged between the large scale direct shear and triaxial test methods. It was concluded that the use of large-scale direct shear testing was a reliable method for determining shear strength parameters for a geocell reinforced soil.

Materials and Methods

Typically, ODOT uses Granular Material Type-C and, textured geofabrics at the MSE wall undercuts. The materials used in this study were procured from ODOT construction sites in Ohio. A summary of the procured materials are provided in the following sections.

Granular Material

The following granular materials were collected from ODOT construction sites for the research, all of which were Type C material.

- Stone A was collected from the Berea Construction.
- Stone B was collected from Wilmington, OH 45177 South of Clinton Field.
(provided by Peter Narsavage).
- Stone C is from Boston Heights. (SR 8 and Turnpike).

<i>Particle Size</i>	<i>% passing</i>
3 inch (75 mm)	100
2 inch (50 mm)	70 to 90
1/2 inch (12.5 mm)	30 to 60
No. 200 (75 μ m)	0 to 13

Table 1: *Type C* granular material specifications.

Since Type C granular material contains up to 3 inch aggregates, the large scale shear was chosen. However, with the 12 inch shear box, only the portion of the Type C material passing through a one inch sieve could be used to comply with the ASTM standards. Because of inadequate sample volume of aggregate A passing through 1 inch sieve, it was combined with aggregate B after all the tests related to it were completed, and named Stone AB.



Figure 2: Granular material obtained from ODOT construction sites.

Geofabrics

Two textured geofabrics, *Geofabric A* and *Geofabric B* were used in the study. *Geofabric A* was obtained from the Berea and Boston Heights, Ohio, sites. *Geofabric B* was obtained from Wilmington, Ohio, site. Specifications of these geofabrics are provided in Appendix B.



Figure 3: Textured Geofabrics A and B used in the research.

Base Soil

The base soils were collected from three construction sites. These soils were labeled as Soil A (Berea site), Soil B (Wilmington site) and Soil C (Boston heights site). The liquid limits (LL) and Plastic limit (PL) of Soil A were determined to be 26 and 15 respectively (ASTM 4318-10). The LL and PL of Soil B were 7 and 5 respectively. More than 85% of Soil A passed through the # 200 sieve. The Soil B had about 65% material passing # 200 sieve. According to the LL and PI index values, Soil A was a clay soil mixed with silt while Soil B was primarily a cohesionless soil composed of silt, with very little clay. The USCS classification for the two soils are as follows:

Soil A: CL

Soil B: ML

Soil C was not used in the study due to time constraints.

Direct Shear Test

A test method for determining the interface shear capacity of geosynthetic reinforced soil was first introduced by ASTM D5321-92, a standard test method for determining the coefficient of soil and geosynthetic or geosynthetic and geosynthetic friction by the direct shear, and then revised by ASTM D5321-02 and ASTM D5321-08. The method is now used to provide the shear parameters of a geosynthetic against soil, or a geosynthetic against another geosynthetic, under a constant rate of deformation.

Large Scale Direct Shear Apparatus

A Large Scale Direct Shear Apparatus (LSDS) with 12 inch square shear box was designed according to ASTM D 5321-08 specifications (Figure 5A). The shear boxes were fabricated at the Cleveland State University machine shop with one inch thick steel plates and mounted on a *Dake Hand Hydraulic Press utility H-frame* with 16 ton capacity (Figure 5). The specifications of the hydraulic press are given in *Appendix A*. The hydraulic press allows a high vertical pressure on the sample during testing. The top shear box was stationary while the bottom shear box had a larger length (15") in the direction of the shear, and mounted on smooth sliding rails. Because of the larger dimension of the bottom shear box, the contact area during the shearing process remained constant and no area correction was required during shear stress calculations.

The lateral force was applied to the bottom box with a manual screw system. The strain rates were maintained between 0.1 to 0.04 inch/min. A digital displacement transducer was attached to this box for measuring the horizontal displacement and a S-type load cell was used to measure the sliding resistance developed at the top shear box. A disc type Loadstar load cell was used for measuring the vertical applied load on the top plate. The load and displacement data was continuously recorded by an *ELE data acquisition* system during the test.

The heights of top and bottom shear boxes were 5 and 4 inch respectively. A one inch thick rigid steel plate was used for applying normal pressure on the top surface of the sample placed in the top shear box.

The developed LSDS shear device is capable of evaluating the shear parameters between a geofabric and soil, stone, or another geofabric by applying and monitoring a wide range of normal and shear loads. Data needed for commercial design, research and quality control can be easily obtained from the setup.

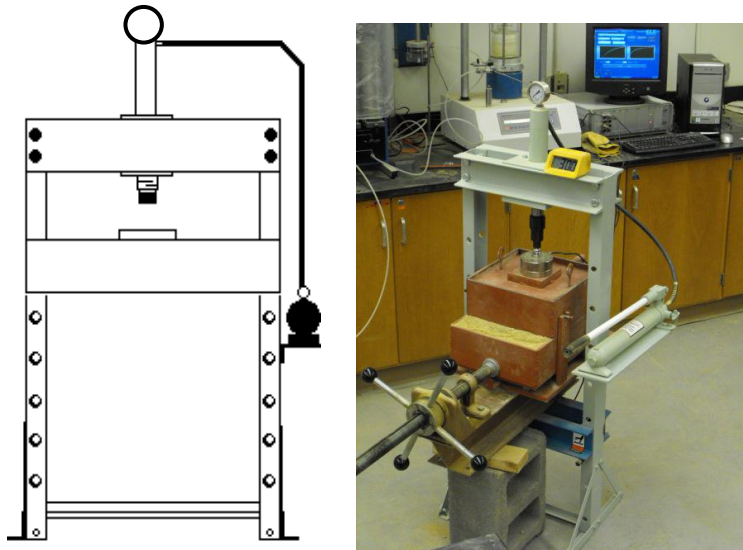


Figure 5: Hydraulic press frame. Figure 5A: Fully assembled photo of LSDS device.

Geofabric Assembly

During the direct shear tests, the geofabrics were oriented such that the shear force was applied across the grains. This was the prevailing ODOT practice of the geofabric placement at the MSE wall undercuts. For assembly in the shear box, the geofabrics were cut carefully to a measured size so that they extended over the edges of the bottom shear box, and securely clamped with seven wing-nuts to the bottom shear box (Figure 6).



Figure 6: The geofabric assembly with seven wing-nuts to the bottom shear box.

Calibration

Before conducting the LSDS tests, the internal shear resistance of the setup was evaluated.

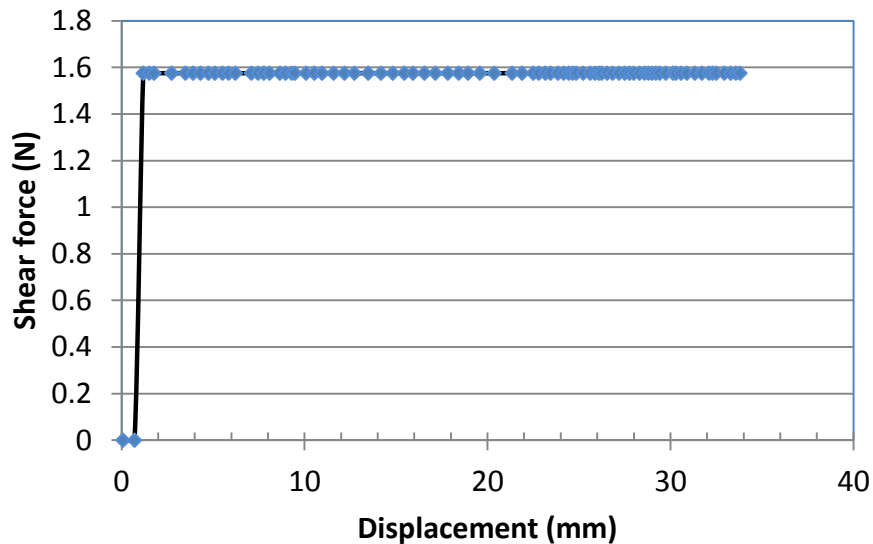


Figure 7: Calibration curve of Large Scale Shear Apparatus for internal frictional resistance.

To determine the system friction, the box assembly was sheared empty with geofabric assembled between the two shear boxes, but without any normal force. Under such conditions, minimal resistance was observed between the shear boxes during the calibration test (Figure 7) and was neglected during shear stress calculations.

Sample Preparation

The base soils were air dried and crushed with a rubber mallet, passed through a # 4 sieve and compacted in the bottom shear box in three layers. The top surface of the compacted clay was brought just above the top edge of the bottom shear box to ensure the shear plane at the intended

location. The aggregates in top box was compacted to about a bulk unit weight of about 105 lb/ft³ and loaded on top with a rigid plate.

When geofabric was used, the aggregates in the top shear box were placed following its assembly over the clay layer in the bottom shear box. The geofabrics were placed with its texture across the shear direction. To prevent crease, the geofabric was clamped such that it was under tension during the tests.

Tests

The initial LSDS tests were conducted with base soils in the bottom shear box, stones in the top shear box and geofabrics at the interface. The geofabrics were then removed from the interface and the tests were repeated. The first set of tests provided friction angles and adhesions between the geofabrics and the stones and the second set provided friction angles and adhesions between the same base soil and stones. The investigation was organized and performed in three phases as shown in Table 2. The shear tests were conducted at normal stress ranges consistent with 30 ft. high MSE walls.

PHASE I						
Bottom Shear Box	Soil A	Soil A	Soil A	Soil A	Soil A	Soil A
Interface	Geofabric A	x	Geofabric A	x	Geofabric A	x
Top Shear Box	Stone B	Stone B	Stone C	Stone C	Stone AB	Stone AB
PHASE II						
Bottom Shear Box	Soil A		Soil A		Soil A	
Interface	Geofabric B		Geofabric B		Geofabric B	
Top Shear Box	Stone B		Stone C		Stone AB	
PHASE III						
Bottom Shear Box		Soil B		Soil B		Soil B
Interface		x		x		x
Top Shear Box		Stone B		Stone C		Stone AB

Table 2: LSDS test scheme for soil/stone and geofabric/stone interfaces.

Data & Analysis

The data from the direct shear tests are shown in the following section. Each set generating the *shear-stress vs normal-stress* correlation was repeated three times and the average shear strength parameters were reported.

Geofabric A/Stone interface properties

The shear stress vs. displacement graphs of *Geofabric A/ Stone B* interface are shown in Figure 8. It is noted that the shear stress did not peak to indicate failure. This is consistent with

behavior of the geofabric interface shear tests reported in literature. The peak shear stress was considered as the failure stress in each case.

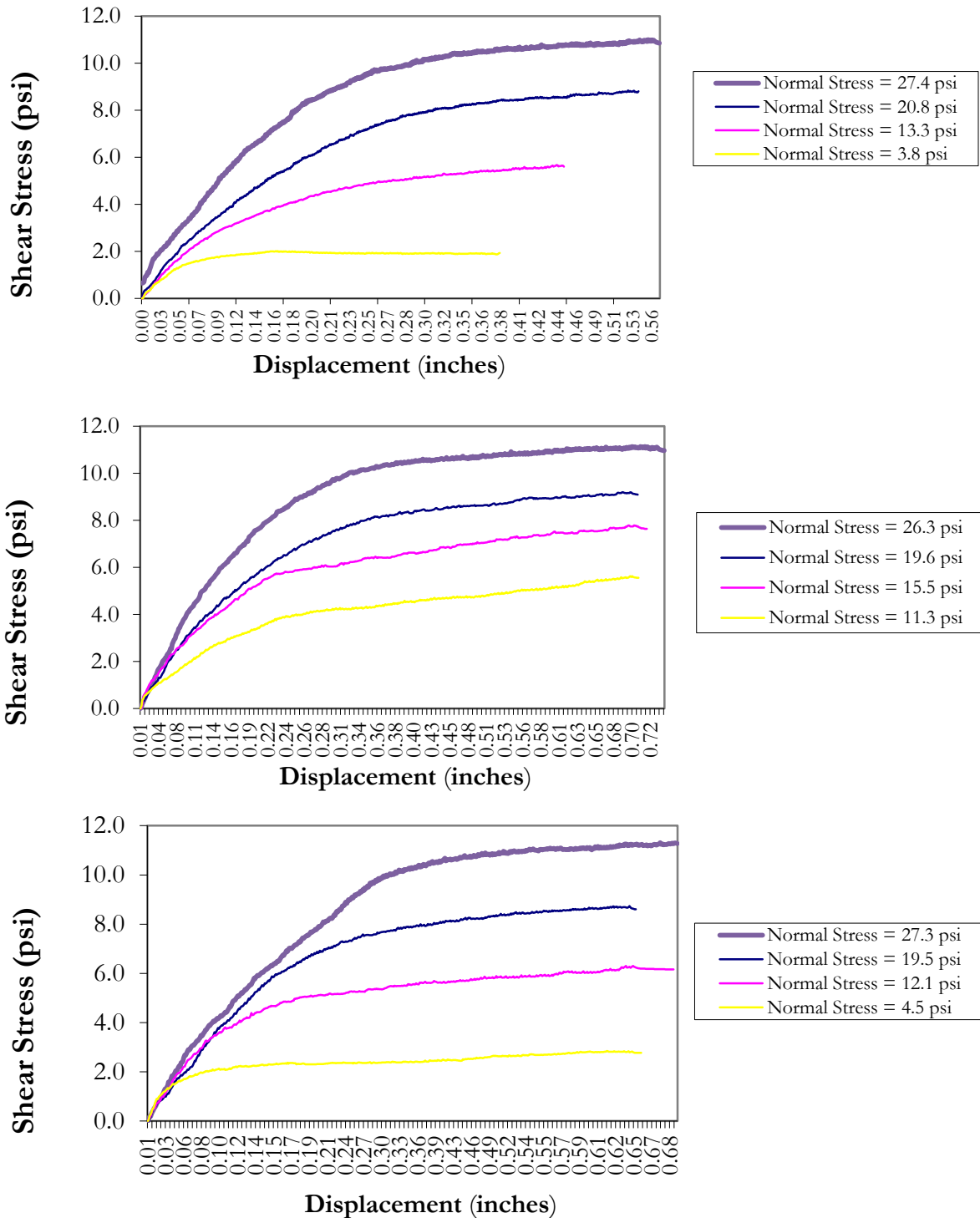


Figure 8: Shear stress vs. displacement for Soil A at bottom, Stone B on top and Geofabric A at interface for TRIALS-1, 2 and 3 respectively.

The plots of maximum shear stress vs. normal stress for the *Geofabric A/Stone B* interface are shown in Figures 9-A. A linear best fit trend line was drawn with *excel spreadsheet* for each case, where y represented shear stress and x represented normal stress. Using the best fit line, the slope angle was calculated as the interface friction angle. A summary of the results are given in Table 3.

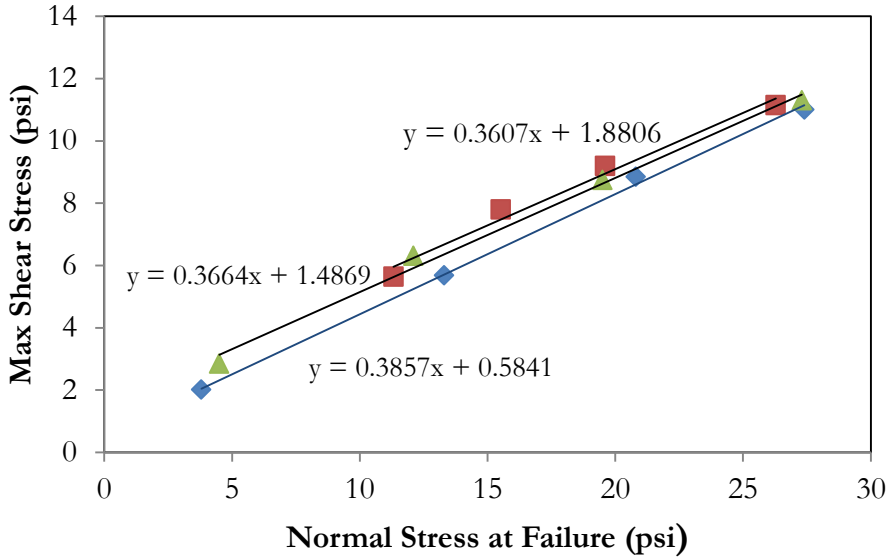


Figure 9 A: Maximum shear stress vs. normal stress for *Geofabric A/ Stone B* interface.

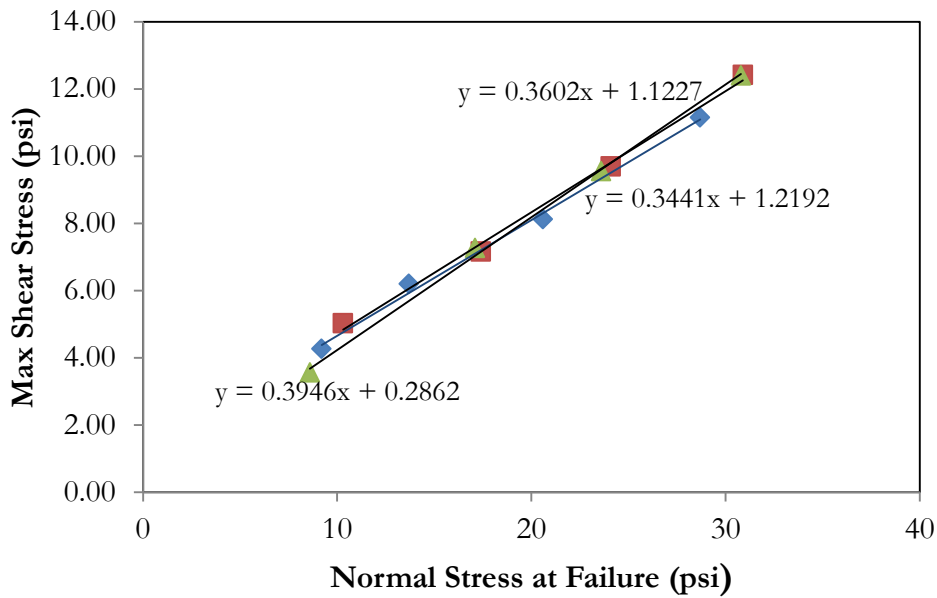


Figure 9 B: Maximum shear stress vs. normal stress for *Geofabric A/ stone C* interface.

Similarly, the shear parameters were determined for *Geofabric A/ Stone C* (Figure 9B), *Geofabric A/ Stone AB* (Figure 9C) interfaces.

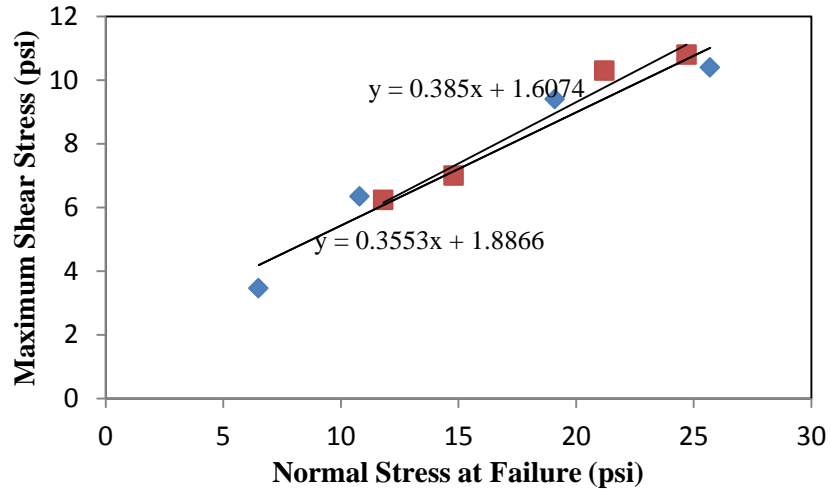


Figure 9 C: Maximum shear stress vs. normal stress for *Geofabric A/ Stone AB* interface.

Soil A/Stone interface properties

The LSDS test results of Soil A interface with Stones B, C and AB are shown in Figures 10 A,B and C. The summary of these results are given Tables 4 and 5.

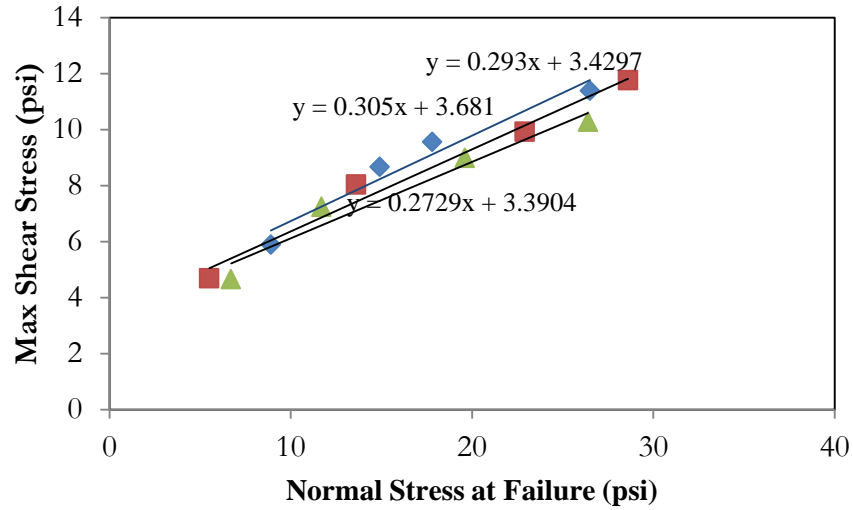


Figure 10 A. Maximum shear stress vs. normal stress for *Soil A / Stone B* interface.

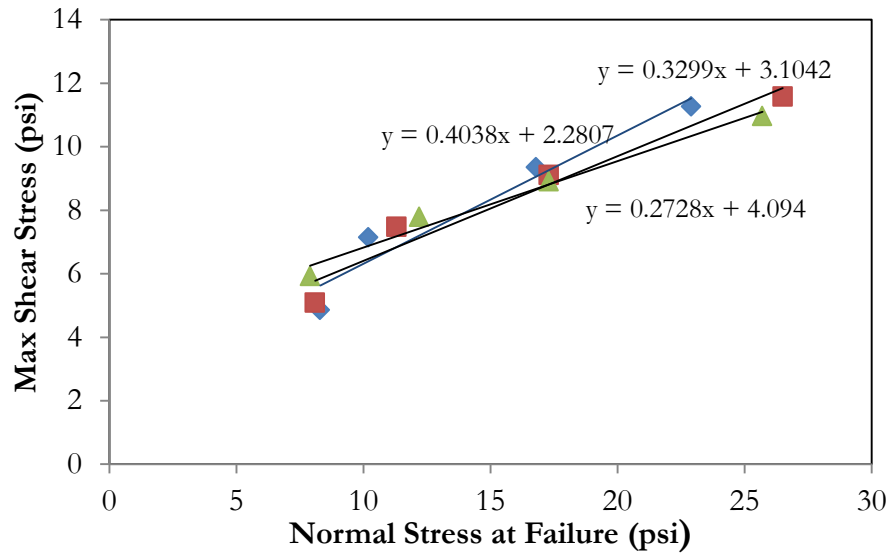


Figure 10 B: Maximum shear stress vs. normal stress for *Soil A / Stone C* interface.

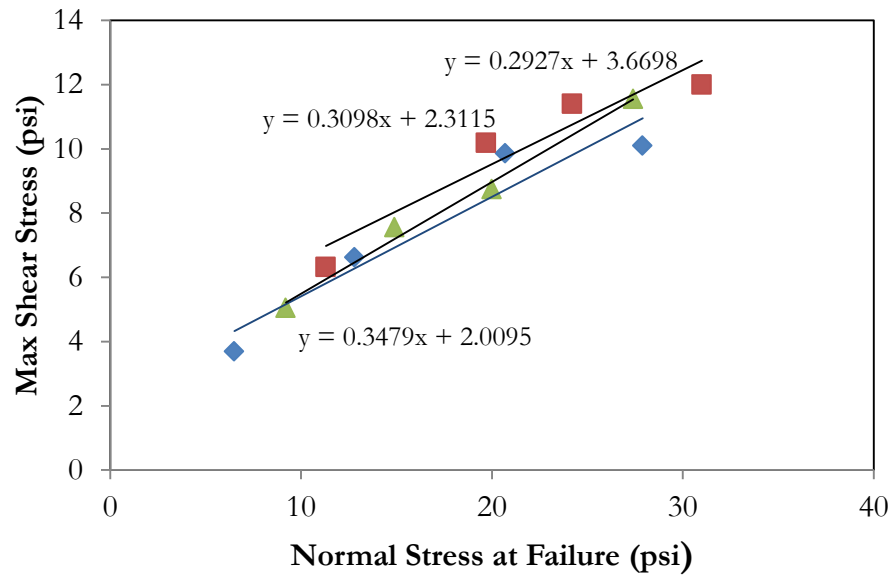


Figure 10 C: Maximum shear stress vs. normal stress for *Soil A / Stone AB* interface.

Trial No.	<i>Geofabric A/ Stone B</i>		<i>Soil A/Stone B</i>	
	Friction angle ϕ°	Adhesion (psi)	Friction angle ϕ°	Adhesion (psi)
1	21.09	0.584	15.26	3.39
2	19.83	1.88	16.96	3.68
3	20.02	1.486	16.33	3.43
<i>Average</i>	20.3	1.27	16.18	3.5

Table 3: Friction angle and adhesion values of Soil A/Stone B, and *Geofabric A/Stone B* interface.

The average shear parameters can be used to write the shear strength equations. For example, the shear strength equations are:

$$\tau = 1.27 + \sigma_n \tan 20.3^\circ \quad \text{psi} \quad [\text{Geofabric A/Stone B interface}]$$

$$\tau = 3.5 + \sigma_n \tan 16.18^\circ \quad \text{psi} \quad [\text{Soil A/Stone B interface}]$$

Trial No.	<i>Geofabric A/ Stone C</i>		<i>Soil A/Stone C</i>	
	Friction angle ϕ°	Adhesion (psi)	Friction angle ϕ°	Adhesion (psi)
1	18.98	1.22	21.98	2.28
2	19.80	1.12	18.25	3.10
3	21.53	0.28	15.25	4.09
<i>Average</i>	20.1	0.87	18.49	3.15

Table 4: Friction angle and adhesion values of Soil A/Stone C, and *Geofabric A/Stone C* interface.

Trial No.	<i>Geofabric A/Stone AB</i>		<i>Soil A/Stone AB</i>	
	Friction angle ϕ°	Adhesion (psi)	Friction angle ϕ°	Adhesion (psi)
1	19.57	1.88	19.18	2.00
2	21.06	1.60	16.31	3.66
3	x	x	17.21	2.31
<i>Average</i>	20.31	1.74	17.56	2.65

Table 5: Friction angle and adhesion values of Soil A/Stone AB, and *Geofabric A/Stone AB* interface.

Geofabric B/Stone interface properties

The LSDS tests were repeated to determine the shear parameters between *Geofabric B* and Stones B, C and AB. The results of these tests are shown the Figures 11 A, B and C, and summaries provided for comparison in Tables 6,7 and 8.

Trial No.	<i>Geofabric B/Stone B</i>		<i>Soil A/Stone B</i>	
	Friction angle ϕ°	Adhesion (psi)	Friction angle ϕ°	Adhesion (psi)
1	21.68	0.6996	15.26	3.39
2	21.07	1.386	16.96	3.68
3	22.93	1.04	16.33	3.43
<i>Average</i>	21.89	1.04	16.18	3.5

Table 6: Friction angle and adhesion values of Soil A/Stone B, and *Geofabric B/Stone B*.

Trial No.	<i>Geofabric B/Stone C</i>		<i>Soil A/ Stone C</i>	
	Friction angle ϕ°	Adhesion (psi)	Friction angle ϕ°	Adhesion (psi)
1	18.71	1.25	21.98	2.28
2	18.26	1.06	18.25	3.10
3	17.29	0.895	15.25	4.29
<i>Average</i>	18.08	1.06	18.49	3.233

Table 7: Friction angle and adhesion values of Soil A/Stone C, and *Geofabric B/Stone C* interface.

Trial No.	<i>Geofabric B/Stone AB</i>		<i>SoilA/Stone AB</i>	
	Friction angle ϕ°	Adhesion (psi)	Friction angle ϕ°	Adhesion (psi)
1	17.42	1.76	19.18	2.00
2	17.61	2.27	16.31	3.66
3	23.99	0.25	17.21	2.31
<i>Average</i>	19.67	1.42	17.56	2.65

Table 8: Friction angle and adhesion values of Soil A/Stone AB, and *Geofabric B/Stone AB* interface.

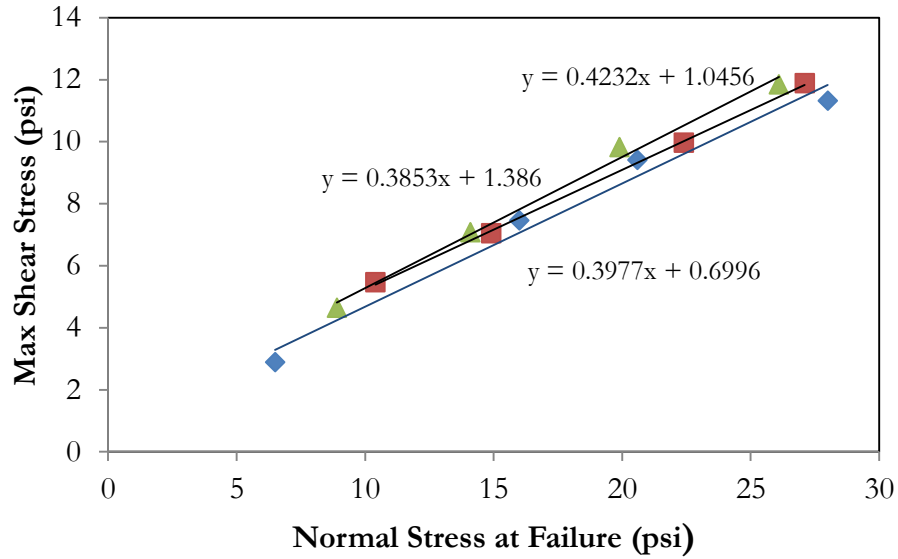


Figure 11 A: Maximum shear stress vs. normal stress for *Geofabric B / Stone B* interface.

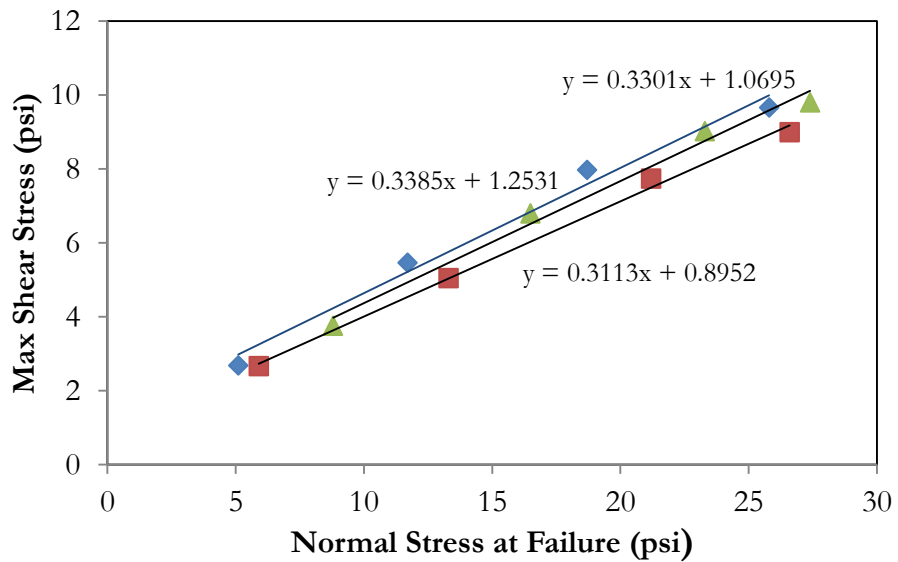


Figure 11 B: Maximum shear stress vs. normal stress for *Geofabric B / Stone C* interface.

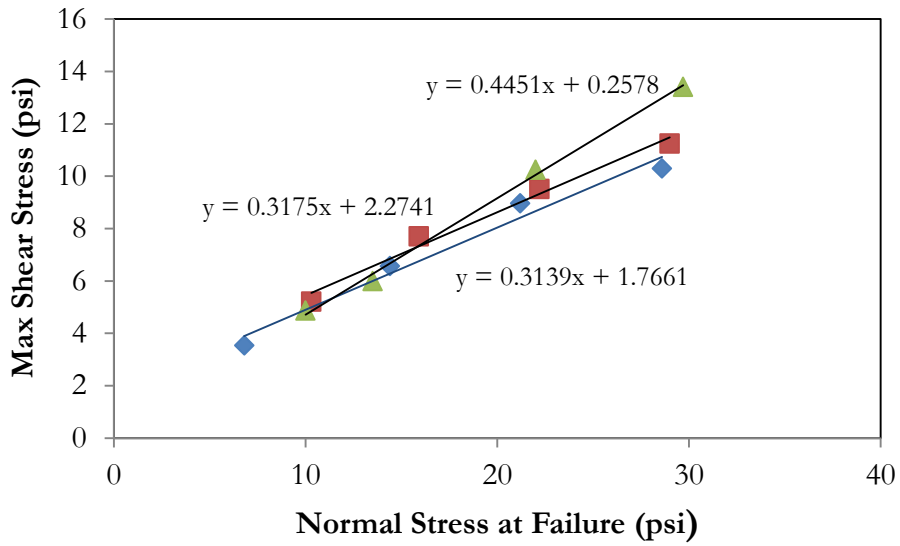


Figure 11 C: Maximum shear stress vs. normal stress for *Geofabric B / Stone AB* interface.

Soil B/Stone interface properties

The tests results for Soil B compacted in the bottom and interchanging Stones B, C and AB in the top shear box are shown in Figures 12 A, B and C. These tests were conducted without any geofabric at the interface. The results of these tests are summarized in Tables 9-14. For comparison purposes the results of geofabric/stone interfaces are also shown in the tables.

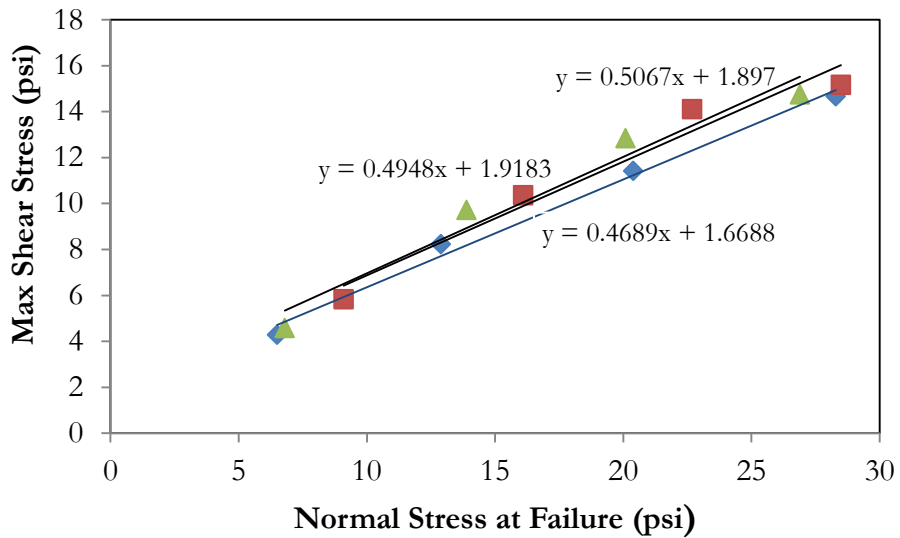


Figure 12 A: Maximum shear stress vs. normal stress for Soil B / Stone B interface.

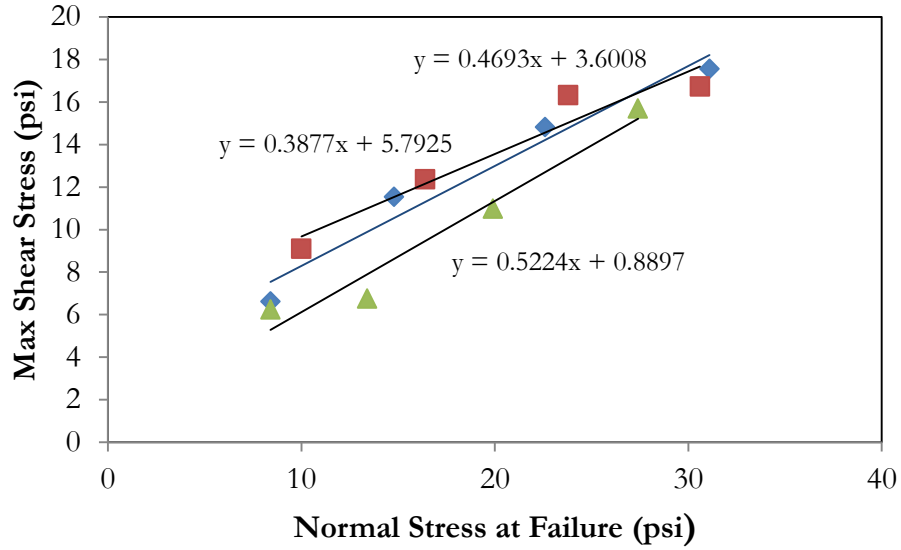


Figure 12 B: Maximum shear stress vs. normal stress for Soil B / Stone C interface.

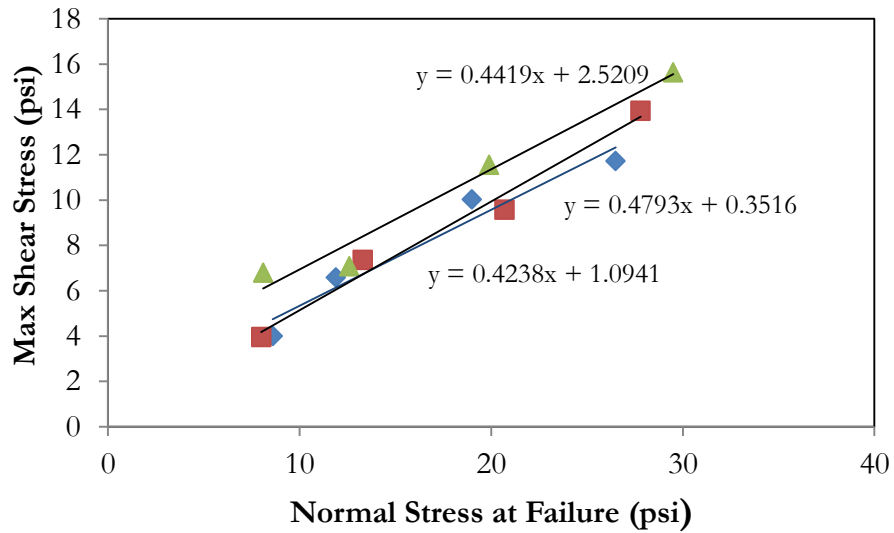


Figure 12 C: Maximum shear stress vs. normal stress for Soil B / Stone AB interface.

Trial No.	<i>Geofabric A/Stone B</i>		<i>Soil B/Stone B</i>	
	Friction angle ϕ°	Adhesion (psi)	Friction angle ϕ°	Adhesion (psi)
1	21.09	0.584	25.11	1.668
2	19.83	1.88	26.32	1.918
3	20.02	1.486	26.87	1.897
<i>Average</i>	20.3	1.27	26.1	1.827

Table 9: Friction angle and adhesion values of Soil B/Stone B, and *Geofabric A/Stone B* interface.

Trial No.	<i>Geofabric A/Stone C</i>		<i>Soil B/Stone C</i>	
	Friction angle ϕ°	Adhesion (psi)	Friction angle ϕ°	Adhesion (psi)
1	18.98	1.22	22.97	1.09
2	19.80	1.12	25.61	0.3516
3	21.53	0.28	23.84	2.52
<i>Average</i>	20.1	0.87	24.14	1.32

Table 10: Friction angle and adhesion values of Soil B/Stone C, and *Geofabric A/Stone C* interface.

Trial No.	<i>Geofabric A/Stone AB</i>		<i>Soil B/Stone AB</i>	
	Friction angle ϕ°	Adhesion (psi)	Friction angle ϕ°	Adhesion (psi)
1	23.2	0.85	25.14	3.6
2	21.06	1.60	21.19	5.79
3	x	x	27.58	0.89
<i>Average</i>	22.13	1.22	24.64	3.42

Table 11: Friction angle and adhesion values of Soil B/Stone AB, and *Geofabric A/Stone AB* interface.

Trial No.	<i>Geofabric B/Stone B</i>		<i>Soil B/Stone B</i>	
	Friction angle ϕ°	Adhesion (psi)	Friction angle ϕ°	Adhesion (psi)
1	21.68	0.6996	25.11	1.668
2	21.07	1.386	26.32	1.918
3	22.93	1.04	26.87	1.897
<i>Average</i>	21.89	1.04	26.1	1.827

Table 12: Friction angle and adhesion values of Soil B/Stone B, and *Geofabric B/Stone B* interface.

Trial No.	<i>Geofabric B/Stone C</i>		<i>Soil B/Stone C</i>	
	Friction angle ϕ°	Adhesion (psi)	Friction angle ϕ°	Adhesion (psi)
1	18.71	1.25	22.97	1.09
2	18.26	1.06	25.61	0.3516
3	17.29	0.895	23.84	2.52
<i>Average</i>	18.08	1.06	24.14	1.32

Table 13: Friction angle and adhesion values of Soil B/Stone C, and *Geofabric B/Stone C* interface.

Trial No.	<i>Geofabric B/Stone AB</i>		<i>Soil B/Stone AB</i>	
	Friction angle ϕ°	Adhesion (psi)	Friction angle ϕ°	Adhesion (psi)
1	17.42	1.76	25.14	3.6
2	17.61	2.27	21.19	5.79
3	23.99	0.25	27.58	0.89
<i>Average</i>	19.67	1.42	24.64	3.42

Table 14: Friction angle and adhesion values of Soil B/Stone AB, and *Geofabric B/Stone AB*.

Discussions

The average friction angles of the *Geofabric A* and Stones B,C and AB were 20.3, 20.1 and 20.31 degrees and the average adhesion values were 1.27, 0.87 and 1.74 psi respectively. The average interface friction between Soil A and the Stones B, C and AB were 16.18, 18.49 and 17.56 degrees with average adhesions of 3.5, 3.23 and 2.65 psi respectively.

Based on a linear Mohr-Coulomb failure criterion, the interface shear strength can be expressed as:

$$\tau = a + \sigma_n \tan \phi$$

where τ is the shear strength, a is the adhesion, σ_n is the normal stress and ϕ is the interface friction angle. The net effects of these changes are shown in Table 15. For Stones B and C, the shear strength decreased (2%, 13.7%), while for stone AB, the shear strength showed slight increase (4%) because of the geofabric. Except for Stone C, the changes were not significant to affect the sliding safety factor ($FS_{sliding}$) of the MSE walls.

	ϕ		a (psi)		τ (psi)	
	Soil A	Geo A	Soil A	Geo A	Soil A	Geo A
Stone B	16.18	20.3	3.5	1.27	10.75371	10.51778
Stone C	18.49	20.1	3.23	0.87	11.59003	10.0187
Stone AB	17.56	20.31	2.65	1.74	10.56126	10.99274

Table 15: Net effect on shear strength of *Geofabric A/stone* interfaces compared to Soil A /stone interfaces with 25 psi normal stress.

For comparison purpose, the failure envelopes of *Soil A/stone* and *Geofabric A/stone* interfaces are shown in Figure 13. It is observed that the failure envelopes for the *Geofabric A/stone* interfaces were lower than the *Soil A/stone* interfaces indicating that the *Geofabric A* had slightly diminished the shear resistance.

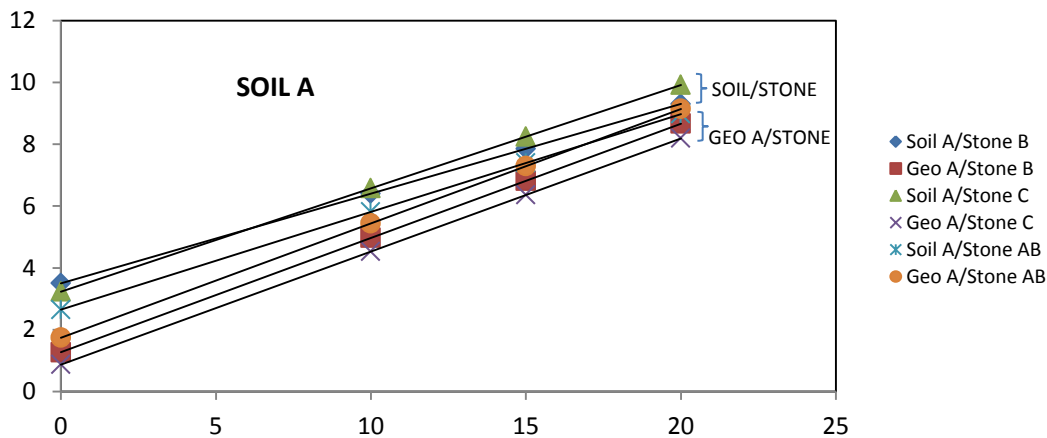


Figure 13: Comparison of maximum shear stress of Soil A interface with stone and *Geofabric A*.

In case of *Geofabric B*, the average friction angles for Stones B, C and AB were 21.89, 18.08 and 19.67 degrees, and the adhesion values were 1.04, 1.06 and 1.42 psi, respectively. The net effect on shear strength is shown in Table 16. It can be seen that in two instances the shear strength had decreased (20% for Stone C and 2% for Stone AB) while on one instance it had increased slightly (3%). The comparison of failure envelopes are shown in Figure 14. The shear behavior of *Geofabric B* with stone interface was very similar to that of *Geofabric A*.

	ϕ		a (psi)		τ (psi)	
	Soil A	Geo B	Soil A	Geo B	Soil A	Geo B
Stone B	16.18	21.89	3.5	1.04	10.75371	11.08487
Stone C	18.49	18.08	3.23	1.06	11.59003	9.221602
Stone AB	17.56	19.67	2.65	1.42	10.56126	10.35653

Table 16: Net effect on shear strength of *Geofabric B/stone* interfaces compared to *Soil A /stone* interfaces with 25 psi normal stress.

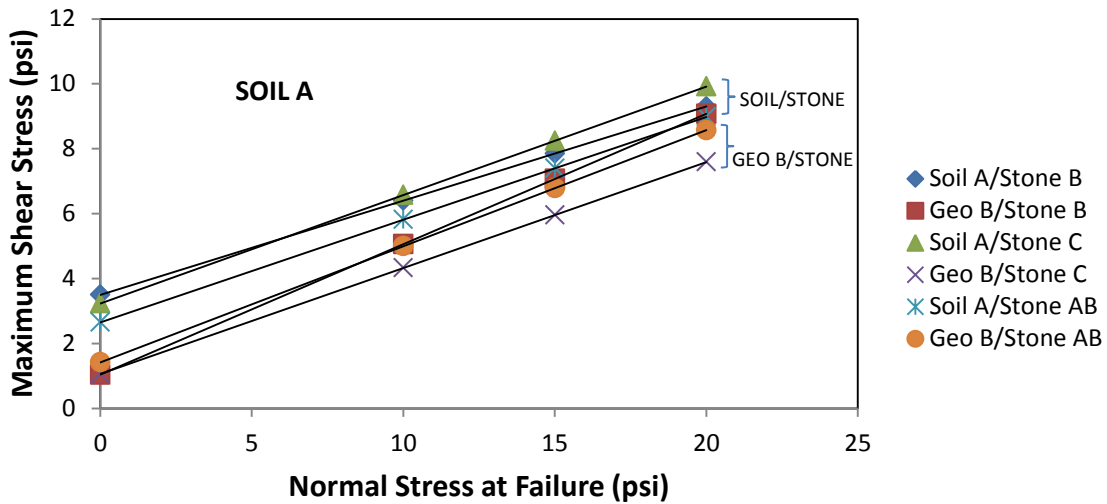


Figure 14: Comparison of maximum shear stress of Soil A interface with stone and *Geofabric B*.

In case of Soil B, the shear parameters with stone interfaces were much higher than those with the geofabric interfaces (Tables 17 and 18). Presence of *Geofabric A* had reduced the shear strengths of Stone B, C & AB interfaces by about 25%, 20% and 26% respectively. In case of *Geofabric B*, the reductions in shear strengths were about 21%, 26% and 30%. These reductions were significant, and could substantially reduce the $FS_{sliding}$ of the MSE walls.

	ϕ		a (psi)		τ (psi)	
	Soil B	Geo A	Soil B	Geo A	Soil B	Geo A
Stone B	26.1	20.3	1.82	1.27	14.06737	10.51778
Stone C	24.14	20.1	1.32	0.87	12.52399	10.0187
Stone AB	24.64	20.31	3.42	1.74	14.88701	10.99274

Table 17: Net effect on shear strength of *Geofabric A/stone* interfaces compared to *Soil B /stone* interfaces with 25 psi normal stress.

	ϕ		a (psi)		τ (psi)	
	Soil B	Geo B	Soil B	Geo B	Soil B	Geo B
Stone B	26.1	21.89	1.82	1.04	14.06737	11.08487
Stone C	24.14	18.08	1.32	1.06	12.52399	9.221602
Stone AB	24.64	19.67	3.42	1.42	14.88701	10.35653

Table 18: Net effect on shear strength of *Geofabric B/stone* interfaces compared to *Soil B /stone* interfaces with 25 psi normal stress.

For comparison purpose, the failure envelopes of the *Soil B/ stone*, *Geofabric A/stone* and *Geofabric B/stone* are shown in figures 15 and 16. It is evident that the *Soil B/stone* interface shear parameters were notably higher than those of the *geofabric/stone* interfaces.

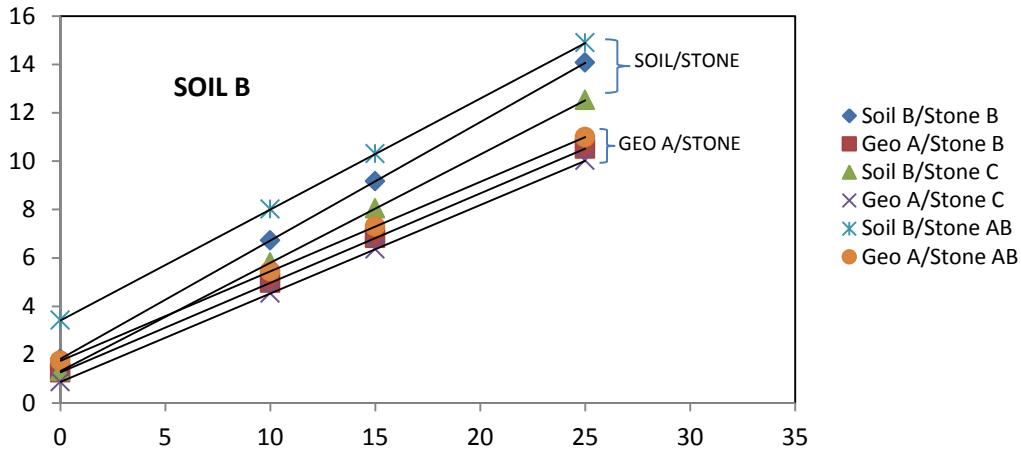


Figure 15: Comparison of maximum shear stress of Soil B interface with stone and *Geofabric B*.

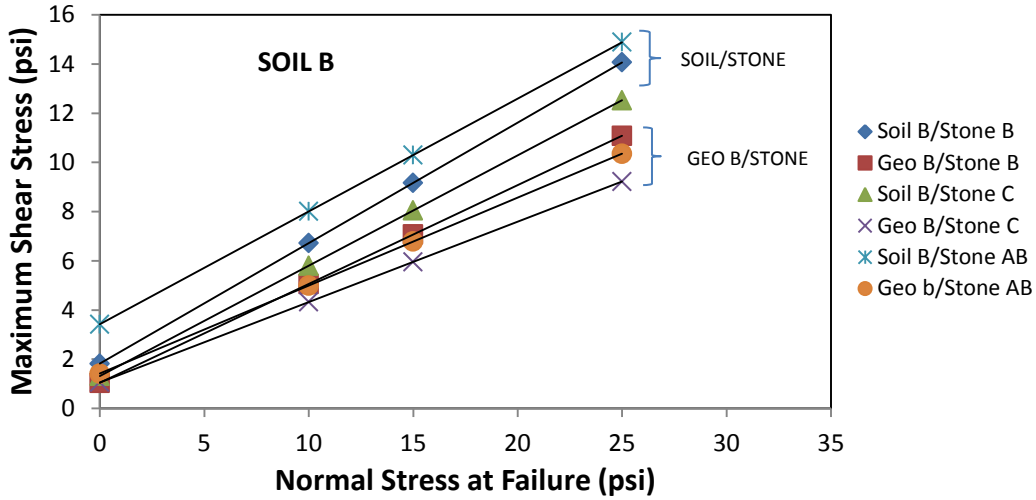


Figure 16: Comparison of maximum shear stress of Soil B with stone and Geofabric B interface.

The test results indicated reduction of shear strength due to the presence of geofabric at the soil/stone interface. The summary of these results are shown in Table 19. The effect was more profound in case of Soil B.

	Soil A	Soil B
Geofabric A	-4%	-24%
Geofabric B	-7%	-26%

Table 19: Reduction of Shear strength for the geofabric/soil Interface compared to the stone/soil interface.

Soil A was primarily a cohesive soil while Soil B was primarily a cohesionless soil. It could therefore be inferred that the effect of geofabric at the undercut is dependent on the nature of the base soil. The results indicate that, in case of a cohesive base soil, the effect of geofabric at the undercut would be perhaps minimal, while in case of sites with cohesionless base soils, the effect of geofabric placement at the undercut could contribute to significant reduction of the interface shear strength.

A study conducted by Nakao and Fitius (2009) demonstrated that small shear box tests were no substitute for large shear box tests, and that downsizing the grading and the size of the sample tested caused the effective friction angle to be under-estimated by as much as 4°. In this research, the Type C material contained particle sizes up to 3 inch and the coarser size fractions above 1 inch were removed prior to testing. This suggests that even though a 12 inch shear box was used to perform the tests, the results could be a slight under-estimate of the true strength of the aggregate tested. Thus the reported friction angles and adhesions are conservative.

Shakir and Zhu (2009) studied the effect of clay moisture content on the interface friction angle between clay and concrete. They reported that the interface shear strength increased with increasing moisture content. The research was conducted under dry conditions and therefore may be regarded as conservative.

Conclusions

The primary conclusion drawn from the project is that the placement of geofabric at the MSE wall undercut adversely affects the shear strength parameters and may reduce the interface shear strength significantly in case of cohesionless base soil and less notably in case of cohesive base soils. Based on the results of the research, the following specific conclusion can be drawn.

- The shear parameters between the soil/stone interfaces were significantly affected by the properties of the base soil. Cohesionless soil generated higher shear resistance at the stone interface than cohesive soils.
- The shear strength parameters at the geofabric/stone interfaces were not affected significantly by the type of stones or the type of geofabrics used in the research.
- For cohesive soil, the shear parameters at the geofabric/stone interface changed from those of the soil/stone interface such that friction angle increased and the adhesion decreased. However, the shear strength at the geofabric interface, calculated with 25 psi normal stress, was slightly lower. Therefore, if the native soil was primarily cohesive, placement of geofabric at the MSE wall undercut would not significantly affect the sliding resistance of the wall.
- For cohesionless soil, the shear parameters at the geofabric/stone interface changed from those of the soil/stone interface such that both, friction angle and adhesion decreased. Therefore, at sites where the native soil was primarily cohesionless, a significant (up to 30% under 25 psi normal pressure) reduction in the shear strength could occur if geofabric was placed at the MSE wall undercut.

Implementation

The valuable insight obtained from this research was that the geofabric at the MSE wall undercut could either increase or decrease the interface friction angle with stone depending on the type of soil present at the base, but, the net effect on the shear strength, with the inclusion of adhesion, was adverse. Up to 30 % reduction in shear strength could occur at the geofabric/soil interface for a 30 ft. MSE wall constructed on cohesionless base soil.

In most instances, the design of MSE walls is dictated by the soil reinforcement lengths (local stability) and the resulting FS_{sliding} (global stability) exceeds the minimum value required by the design. Nonetheless, the findings of this research indicate that the design of MSE walls with geofabric at the undercut may require modification of the sliding safety factor to reflect the reduced shear strength at the interface. A conservative suggestion is to calculate the FS_{sliding} by reducing the shear strengths by 70 % and 85% for cohesionless and cohesive base soils respectively. Depending on the site conditions, this modification might not affect the final design at the end.

It should be kept in mind that the results of this research are applicable only to the materials used in this investigation and should not be generalized to field conditions with different materials.

Acknowledgements

The authors are grateful to Mr. Peter Narsavage for providing the samples and his valuable guidance during the project. The authors are also grateful to Dr. Jawdat Siddiqi and Dr. Bashr Altarawneh, for their valuable inputs and to Ms. Vicky Fout for coordinating the project.

REFERENCES

- AASHTO Designation T 236-72. "Standard Test Method for Direct Shear Test of Soils Under Consolidated Drained Conditions."
- ASTM D3080. "Standard Test Method for Direct Shear Test of Soils Under Consolidated Drained Conditions."
- ASTM D5321-08. "Standard Test Method for Determining the Coefficient of Soil and Geosynthetic or Geosynthetic and Geosynthetic Friction by the Direct Shear Method."
- Design reference for Interface Shear Box (Large Scale). Source: <http://www.durhumgeo.com/testing/geosynthetics/interface-shear-box>. Last accessed May 24, 2009.
- Narsavage, Peter. "ODOT Design and construction Requirements for MSE Walls." Power Point Presentation, Ohio Transportation Engineering Conference, 2006.
- State of Ohio Department of Transportation Supplemental Specification 840 - Mechanically Stabilized Earth Walls. January 19, 2007.
- U.S. Department of Transportation Federal Highway Administration. Chapter 2. Direct Shear Testing, Evaluation of LS-DYNA Soil Material Model 147. Publication No. FHWA-HRT-04-094. November 2004. Source: <http://www.tfhr.gov/safety/pubs/04094/02.cfm>. Last accessed May 24, 2009.

- U.S. Department of Transportation Federal Highway Administration. "Mechanically Stabilized Earth Walls and Reinforced Soil Slopes Design and Construction Guidelines." National Highway Institute Office of Bridge Technology. Publication No. FHWA-NHI-00-043. March 2001.
- Wang Yi-min, Chen Ye-kai, Lui Wei. "Large-Scale Direct Shear Testing of Geocell Reinforced Soil." *Journal of Central South University of Technology*. Volume 15, Number 6, 2008. Pgs.895-900.
- Tomoyo Nakao and Stephen Fityus, "Direct Shear Testing of a Marginal Material Using a Large Shear Box", *Geotechnical Testing Journal*, Vol. 31, No. 5, 2009
- R. R. Shakir and Jungao Zhu, "Behavior of compacted clay-concrete interface" *Front. Archit. Civ. Eng. China* 2009, 3(1): 85– 92
- Hausmann, M., 1990, *Engineering Principles of Ground Modification*, McGraw-Hill, New York.

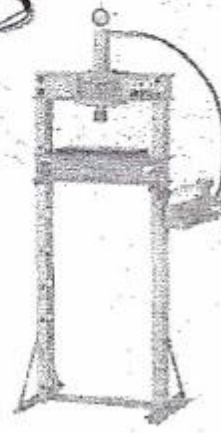
APPENDIX - A

Hand Hydraulic Presses **DAKE®**

Utility H-Frame

- Single speed hand pump with adjustable mounting • Top mounted gage
- B-10: bench mounted • F-10: floor mounted
- Includes: frame, table plate and v-blocks, flat ram nose and step reduced ram nose

Mr's #	72200	72210
Desc.	B-10 Bench Mount	F-10 Floor Mount
Force Pressure (Tons)	10	10
Distance Between Uprights (In.)	16¾	16¾
Minimum Ram to Table (In.)	4	38
Maximum Ram to Table (In.)	16	38
Ram Travel (In.)	6	6
Base Width (In.)	23	24
Base Depth (In.)	18	28
Overall Height (In.)	36	60
Weight (Lbs.)	132	167
Order #	93143063	93143071
Price Ea.	\$273.00	\$390.00



APPENDIX - B

Geofabric A

Berea Site A & Boston Heights Site C



Product Data Sheet
GTF 404

A woven geotextile filter fabric, produced from high-tenacity polypropylene monofilament yarns. GTF404 is typically used in Subsurface Drainage or Permanent Erosion Control applications. GTF 404 has been UV stabilized and packaged in conformance with ASTM D4873.

PROPERTY	TEST PROCEDURE	METRIC		ENGLISH	
		MARV		MARV	
Grab Tensile Strength (W/F)	ASTM D-4632	1760 / 1402	N	400 / 315	lbs
Grab Elongation	ASTM D-4632	15/15	%	15/15	%
Wide Width Tensile	ASTM D-4595	43.8/40.3	kN/m	250/230	lbs/in
Trapezoid Tear	ASTM D-4533	668 / 704	N	150 / 165	lbs
Puncture	ASTM D-4833	668	N	150	lbs
CBR Puncture	ASTM D-6241	5118	N	1150	lbs
Permittivity	ASTM D-4491	0.900	sec ⁻¹	0.900	sec ⁻²
A.O.S.	ASTM D-4751	0.425	mm	40	U.S. Sieve
UV Resistance (500 hrs)	ASTM D-4355	90	%	90	%
Water Flow Rate	ASTM D-4491	2852	lpm/m ²	70	gpm/ft ²
Percent Open Area	CW02215	1	%	1	%

VOLUME	TEST PROCEDURE	METRIC		ENGLISH	
		Typical		Typical	
Weight	ASTM D-5261	271	g/m ²	8.0	oz/yd ²
Thickness	ASTM D-5199	.889	mm	35	mils

PACKAGING	METRIC			ENGLISH		
	AREA	WIDTH	LENGTH	AREA	WIDTH	LENGTH
Roll sizes	418 m ²	4.57 m	91.4 m	500 yd ²	15'	300'

This information relates to the specific material designated and may not be valid for such material used in combination with any other materials or in any process. Such information is, to the best of our knowledge and belief, accurate and reliable as of the date compiled. However, no representation, warranty or guarantee is made as to its accuracy, reliability or completeness. It is the user's responsibility to satisfy himself or herself as to the suitability and completeness of such information for his or her own particular use. We do not accept liability for any loss or damage that may occur from the use of this information, nor do we offer any warranty against infringement.

LINQ and the Thrace-LINQ emblem are registered trademarks of Thrace-LINQ, Inc.

Thrace-LINQ, Inc

2550 West Fifth North St., Summerville, SC 29483
1-800-445-6675

11/5/2008

Geofabric B

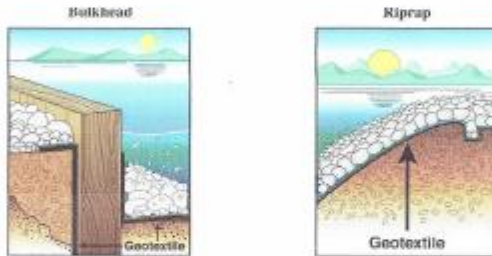


Geo B
US 670

3904 Virginia Ave • Cincinnati, Ohio 45227 • Phone (513) 271-6000 • Fax (513) 271-4420

Woven Filtration

A Woven Calendared Monofilament Filtration Geotextile made of 100% Polypropylene Yarns. This product is specifically designed for drainage and filtration applications. Having a *Percent Open Area* of 4 – 6%, gives this product excellent hydraulic properties, while reducing the chances of clogging.



PROPERTY	TEST METHOD	ENGLISH	METRIC
Tensile Strength	ASTM D-4632	370 x 250 lbs	1650 N x 1110 N
Elongation @ Break	ASTM D-4632	15 %	15 %
Mullen Burst	ASTM D-3786	480 psi	3300 kPa
Puncture Strength	ASTM D-4833	120 lbs	534 N
Trapezoidal Tear	ASTM D-4533	100 x 60 lbs	445 N x 267 N
Apparent Opening Size	ASTM D-4751	70 US Sieve	0.212 mm
Permittivity	ASTM D-4491	0.28 Sec ⁻¹	0.28 Sec ⁻¹
UV Resistance, % Retained	ASTM D-4355	90 %	90 %
Percent Open Area	CWO-22125	4 - 6%	4 - 6%
Flow Rate	ASTM D-4491	18 gal/min/sf	733 l/min/m ²

The above information is to the best of our knowledge accurate, but is not intended to be considered as a guarantee. Any implied warranty for a particular use or purpose is excluded. If the Product does not meet the above properties, and notice is given to US Fabrics, Inc., the product will be replaced or refunded. (1/2005)